JOURNAL OF THE ROYAL SOCIETY Interface

J. R. Soc. Interface (2012) **9**, 880–889
doi:10.1098/rsif.2011.0387
Published online 12 October 2011

Influence of strontium for calcium substitution in bioactive glasses on degradation, ion release and apatite formation

Yann C. Fredholm[1], Natalia Karpukhina[3], Delia S. Brauer[3,*], Julian R. Jones[1], Robert V. Law[2] and Robert G. Hill[3]

[1]*Department of Materials, and* [2]*Department of Chemistry, Imperial College London, Exhibition Road, London SW7 2AZ, UK*
[3]*Unit of Dental Physical Sciences, Barts and The London School of Medicine and Dentistry, Queen Mary University of London, Mile End Road, London E1 4NS, UK*

Bioactive glasses are able to bond to bone through the formation of hydroxy-carbonate apatite in body fluids while strontium (Sr)-releasing bioactive glasses are of interest for patients suffering from osteoporosis, as Sr was shown to increase bone formation both *in vitro* and *in vivo*. A melt-derived glass series (SiO_2–P_2O_5–CaO–Na_2O) with 0–100% of calcium (Ca) replaced by Sr on a molar base was prepared. pH change, ion release and apatite formation during immersion of glass powder in simulated body fluid and Tris buffer at 37°C over up to 8 h were investigated and showed that substituting Sr for Ca increased glass dissolution and ion release, an effect owing to an expansion of the glass network caused by the larger ionic radius of Sr ions compared with Ca. Sr release increased linearly with Sr substitution, and apatite formation was enhanced significantly in the fully Sr-substituted glass, which allowed for enhanced osteoblast attachment as well as proliferation and control of osteoblast and osteoclast activity as shown previously. Studying the composition–structure–property relationship in bioactive glasses enables us to successfully design next-generation biomaterials that combine the bone regenerative properties of bioactive glasses with the release of therapeutically active Sr ions.

Keywords: bioactive glass; strontium; apatite; ion release; osteoporosis; bone regeneration

1. INTRODUCTION

In osteoporotic bone, osteoclasts resorb too much bone, while osteoblastic bone formation is not sufficient to counterbalance this, resulting in reduced bone mineral density. This leads to weak and brittle bones, which can break easily even during everyday activities. Typical sites for osteoporotic fractures are hip, spine, forearm and humerus, and women in western Europe over the age of 50 were shown to have a 47 per cent likelihood of fractures during their remaining lifetime [1]. In 2000, the number of osteoporotic fractures in Europe was estimated to be nearly 3.8 million, causing an estimated total cost of 31.7 billion euros [2]. Strontium (Sr) ions have been shown to stimulate osteoblastic bone formation and to inhibit osteoclastic bone resorption both *in vitro* and *in vivo* [3,4]. Indeed, strontium ranelate (Protelos) is a drug approved for treatment and prevention of osteoporosis [5,6], whereas Sr-containing bioactive glasses were shown to combine the known bone regenerative properties of bioactive glasses with the anabolic and anti-catabolic effects of Sr cations *in vitro* [7].

Bioactive glasses undergo surface reactions and form a layer of hydroxy-carbonate apatite (HCA) on their surface when exposed to body fluids. These glasses are being used as bone substitute materials as they promote bone formation and osseointegration [8,9]. The HCA surface layer is thought to play a critical role for attachment of proteins such as fibronectin and vitronectin, which osteoblasts bind to and proliferate on [10], thereby allowing for the formation of an intimate bond to bone. Bioactive glasses also release ions that promote the osteoblast phenotype [11,12], and new compositions can be tailored to release specific ions to address clinical needs.

We have recently shown that Sr-substituted bioactive glasses are promising as bone repair and regeneration therapies with benefits comparable with those of strontium ranelate [7], making Sr-containing bioactive glasses a promising material for bone substitution and therapeutic release of Sr ions. We have also shown that when Sr is substituted for Ca on a

*Author for correspondence (d.brauer@qmul.ac.uk).

Received 16 June 2011
Accepted 22 September 2011

Table 1. Nominal glass composition (mol%) and molar strontium for calcium substitution (%).

glass	Sr for Ca substitution	SiO_2	P_2O_5	CaO	SrO	Na_2O
Sr0	0	49.47	1.07	23.08	—	26.38
Sr2.5	2.5	49.47	1.07	22.50	0.58	26.38
Sr10	10	49.47	1.07	20.77	2.31	26.38
Sr50	50	49.47	1.07	11.54	11.54	26.38
Sr100	100	49.47	1.07	—	23.08	26.38

molar base, the glass network expands owing to the larger ionic radius of Sr compared with Ca [13]. Here, we present a detailed study of dissolution, ion release and apatite formation of bioactive glasses in the system $49.46\,SiO_2 - 1.07\,P_2O_5 - (23.08\text{-}X)$ CaO-X SrO-$26.38Na_2O$ ($X = 0$–23.08), showing how the structural changes caused by Sr substitution significantly alter the *in vitro* behaviour of the glasses.

2. MATERIAL AND METHODS

2.1. Glass synthesis

Glasses in the system SiO_2–P_2O_5–CaO–SrO–Na_2O were prepared using a melt–quench route. Zero, 2.5, 10, 50 and 100 per cent of Ca were replaced by Sr on a molar base (glasses Sr0–Sr100; table 1) in order to maintain the structure of the silicate glass matrix [14]. Mixtures of analytical grade SiO_2 (Prince Minerals Ltd, Stoke-on-Trent, UK), P_2O_5, $CaCO_3$, $SrCO_3$ and Na_2CO_3 (all chemicals from Sigma-Aldrich, Gillingham, UK) were melted in a platinum–rhodium crucible for 1.5 h at 1400°C in an electric furnace (Lenton, Hope Valley, UK). A batch size of approximately 100 g was used. After melting, the glasses were rapidly quenched into water to prevent crystallization. After drying, the glass was ground using a vibratory mill (Gyro Mill, Glen Creston, London, UK) for 7 min and sieved to a particle size below 38 μm. The amorphous structure of the glasses was confirmed by powder X-ray diffraction (XRD) as shown previously [13].

Glass monoliths were produced by re-melting glass frit for 30 min at 1450°C, pouring the melt into a pre-heated graphite mould and placing the moulds in a furnace pre-heated to 550°C. The glass was then allowed to cool slowly to room temperature in a furnace overnight. The rods were cut into 1 mm thick discs using a low-speed diamond saw (IsoMet, Buehler GmbH, Düsseldorf, Germany).

2.2. pH and ion release in simulated body fluid and Tris buffer

Simulated body fluid (SBF) was prepared using 7.996 g sodium chloride, 0.350 g $NaHCO_3$, 0.224 g potassium chloride, 0.228 g $K_2HPO_4 \times 3H_2O$, 0.305 g $MgCl_2 \times 6H_2O$, 0.368 g $CaCl_2 \times 2H_2O$, 0.071 g sodium sulphate and 6.057 g tris(hydroxymethyl)amino methane, $(CH_2OH)_3CNH_2$, (Tris) per litre SBF. The pH was adjusted to 7.25 using 1 N hydrochloric acid (all chemicals from Sigma-Aldrich) as described by Kokubo *et al.* [15] using a pH meter (Oakton Instruments, Nijkerk, The Netherlands).

Tris buffer solution was prepared by dissolving 15.090 g Tris in *ca* 800 ml deionized water, adding 44.2 ml 1 M hydrochloric acid, heating to 37°C over night, adjusting the pH to 7.25 using 1 M hydrochloric acid and filling to a total volume of 2000 ml using deionized water. Both solutions were kept at 37°C.

Fifty millilitres SBF were pipetted into 150 ml PE bottles, and 75 mg of glass powder (less than 38 μm) were dispersed in the solution, corresponding to a concentration of 1.5 g l^{-1}. Experiments were performed in duplicate. Samples were placed in an orbital shaker at 37°C at an agitation rate of 60 r.p.m. for 5, 15, 30, 60, 120, 240 and 480 min. At the end of each time period, the pH was measured and the solution filtered through medium porosity filter paper (5 μm particle retention, VWR International, Lutterworth, UK), stored at 4°C and analysed by inductively coupled plasma optical emission spectroscopy (Thermo FI ARL 3580 B). Glass powder treated in SBF was rinsed with acetone to stop any further reaction. Studies in Tris were performed in an analogous fashion. Glass discs were immersed in SBF for 1 week at 37°C.

2.3. Characterization of glass powders after immersion in simulated body fluid

Filter paper with retained SBF-treated powders was dried at 37°C, and the dried powders were analysed using Fourier-transform infrared spectroscopy (FTIR; Spectrum GX, Perkin-Elmer, Waltham, MA, USA) and XRD (Philips PW 1700, Leiden, The Netherlands; 40 kV/40 mA, CuKα, data collected at room temperature).

2.4. Scanning electron microscopy

Glass discs treated in SBF were mounted in epoxy resin, cross-sectioned, and polished and characterized in a scanning electron microscope (SEM; JSM-840A, JEOL, Tokyo, Japan) using secondary and back-scattered electrons modes at 15 kV on polished cross sections of glass discs. Energy-dispersive X-ray spectroscopy analysis (EDX) was carried out to determine the composition of the different layers observed as a function of the distance from the surface.

2.5. Solid-state nuclear magnetic resonance spectroscopy

Glass powders before and after immersion in SBF were analysed using ^{31}P magic angle spinning nuclear magnetic resonance (MAS-NMR) on a Bruker 200 MHz (4.7 T) spectrometer. ^{31}P MAS-NMR spectra were collected at 81.0 MHz in a 4 mm rotor spinning at about

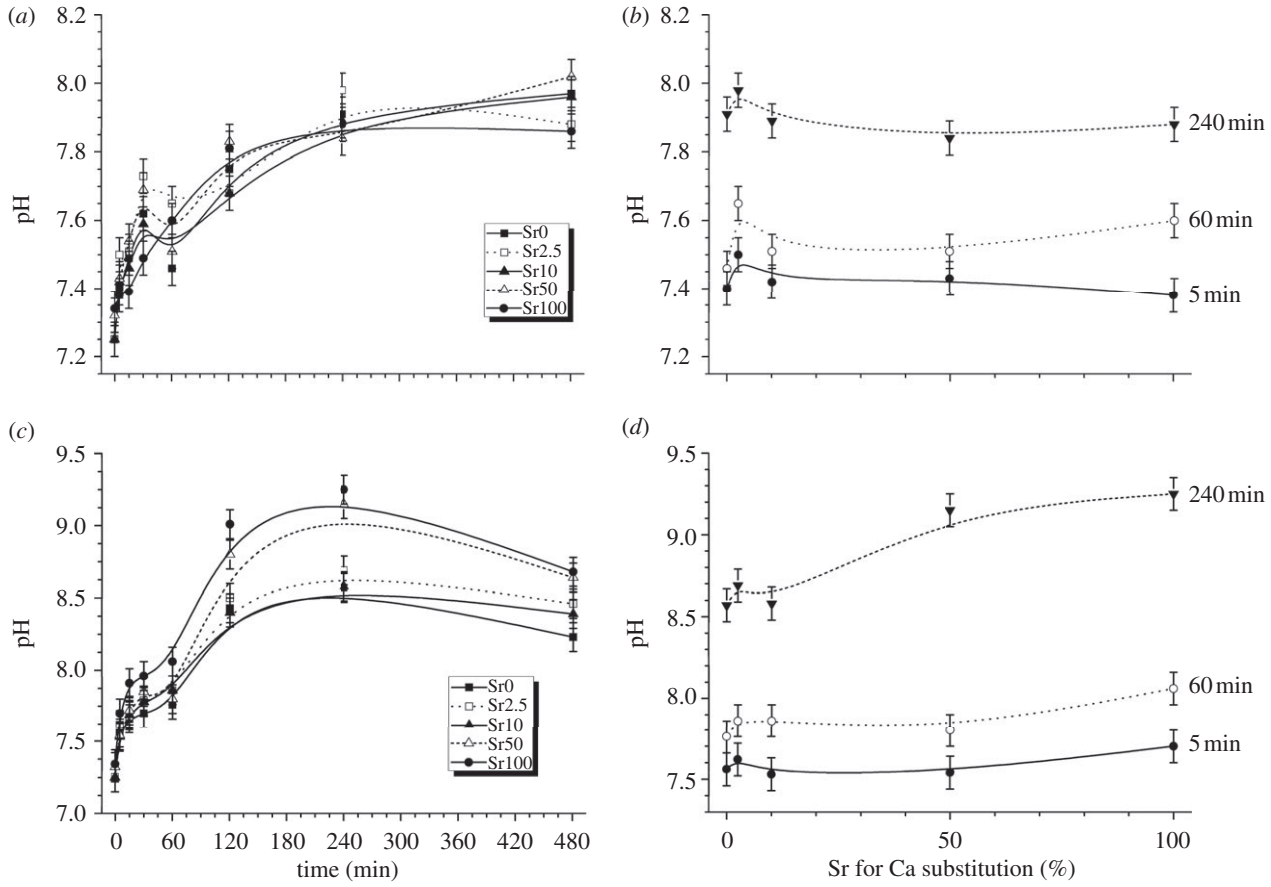

Figure 1. pH changes of (*a*,*b*) Tris buffer and (*c*,*d*) SBF after immersion of glass powders. (Lines are drawn as a guide to the eye.)

5 kHz with a 30 s recycle delay and eight scans before counting. ^{31}P chemical shift was referenced to 85% H_3PO_4.

3. RESULTS AND DISCUSSION

3.1. pH changes and ion release in Tris buffer and simulated body fluid

The glasses showed a pronounced pH rise upon immersion in both Tris buffer and SBF (shown in figure 1*a*,*c*), which is a typical effect of bioactive glasses [16] and is known to aid apatite formation [17,18]. The pH increased with time for all the glasses, but there was a slight reduction in pH at 480 min in SBF, while no such pH decrease was observed in Tris buffer. The reduction in pH in SBF is likely to be caused by the formation of carbonates once all phosphate ions have been consumed for apatite formation, and this was confirmed by a strong carbonate absorption band in the FTIR studies and the observation of a strong diffraction line for a mixed Sr/Ca carbonate in the XRD patterns discussed later. Owing to a larger buffering capacity of the Tris buffer used, the overall pH change in Tris buffer was less than in SBF.

pH in SBF also showed a correlation with Sr substitution, with pH increasing for increasing Sr content in the glass (figure 1*d*). As the glass powders all had particle size distributions in the same range (results not shown), the greater pH increase found with increasing Sr substitution indicates an increase in dissolution rate of the glasses, which can be explained on the basis of the more weakly bonded and more expanded network observed previously [13]. A fixed amount of glass (75 mg) was used in these experiments; however, the atomic weight of Sr is 87 compared with 40 g mol^{-1} for Ca. As a result, the molar amount of glass decreased with increasing Sr substitution, and a reduced pH rise with increasing Sr would have been expected if the glasses all dissolved at the same rate.

Figure 2 shows the Ca, phosphorus, silicon and Sr release into Tris buffer and SBF as a function of time. Elemental concentrations of Ca, silicon and—with increasing Sr content in the glass—Sr and phosphorus in Tris buffer increased with time. Figure 3*a* shows the Sr release to be directly proportional to the Sr content in the glass, an effect that is observed at all time points. While the decrease in Ca release with increasing Sr (i.e. decreasing Ca) in the glass is linear for Sr substitutions of 10 per cent or above, we see an increase in Ca release for 2.5 per cent substitution (Sr2.5) despite the fact that the Ca content in the glass is reduced. Figure 3*b* (accounting for the differences between Ca and Sr in atomic weight as discussed earlier) confirms this effect. It is thought to be a result of the effect Sr has on the glass structure, as substituting even small amounts of Sr for Ca expands the glass network [13] owing to the larger ionic radius of Sr (1.16 Å) compared with Ca (0.94 Å). The effect on solubility, however, seems to become less pronounced for larger Sr for Ca substitution.

Phosphate release increased with increasing Sr for Ca substitution (figure 3*a*), whereas silicon and combined

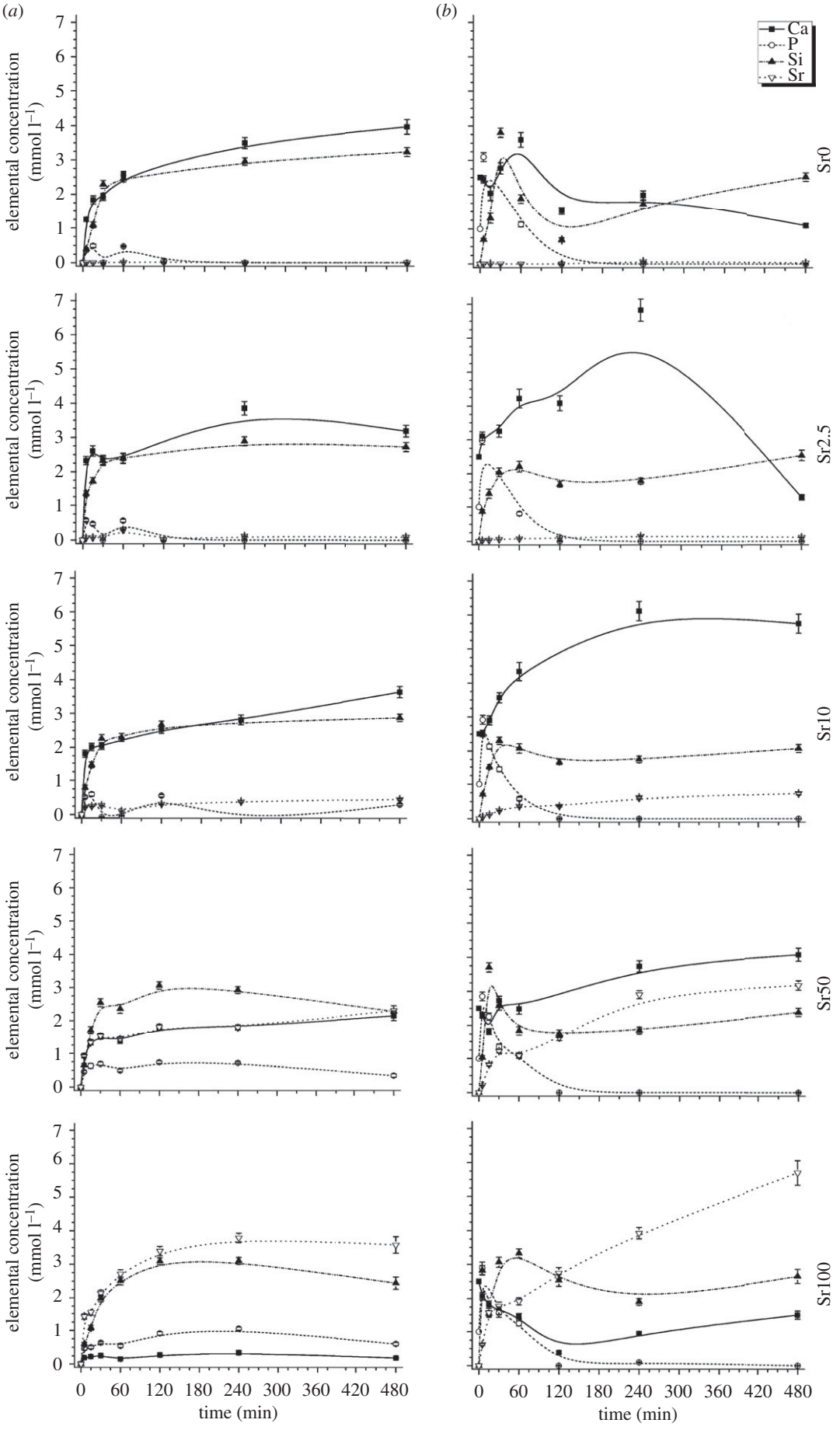

Figure 2. Elemental concentrations in (*a*) Tris buffer and (*b*) simulated body fluid (SBF) over time for glasses with 0, 2.5, 10, 50 and 100% strontium for calcium substitution (from top to bottom). (Lines are drawn as a guide to the eye.)

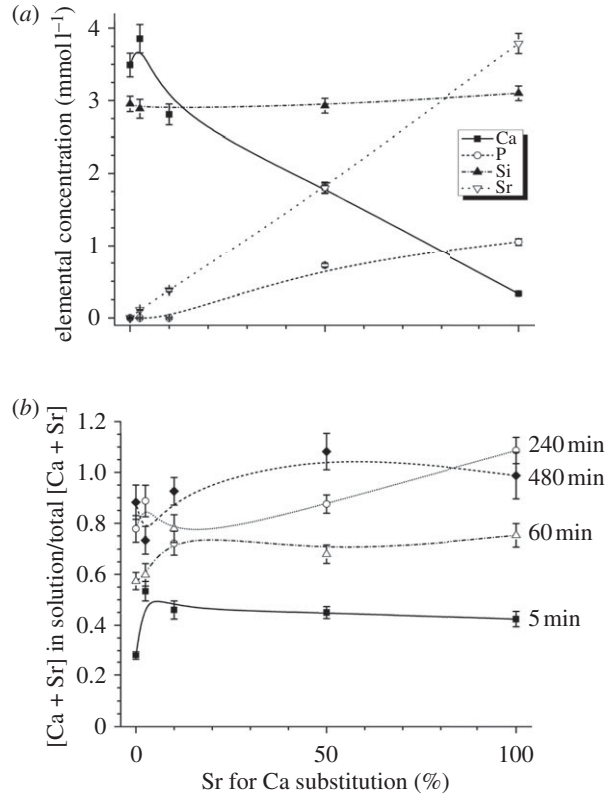

Figure 3. (*a*) Elemental concentrations of Ca, P, Si and Sr as a function of Sr for Ca substitution at 240 min in Tris buffer; (*b*) combined dissolved Ca and Sr relative to their total amount as a function of Sr for Ca substitution in the glass at various time points. (Lines are drawn as a guide to the eye.)

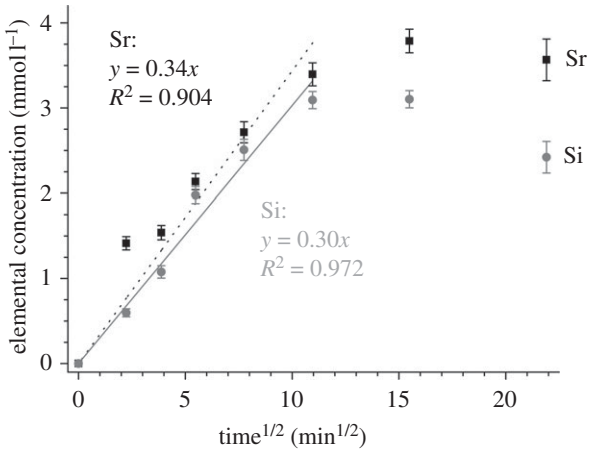

Figure 4. Strontium (black squares) and silicon (grey circles) concentrations in Tris buffer as a function of square root of time suggesting a two-step degradation mechanism, with initial dissolution controlled by diffusion (linear). (Lines are linear regression of dissolution data from 5 to 120 min.)

Ca + Sr concentrations remained constant. This, again, could be caused by the more expanded and more easily degradable silicate network [13], which facilitates dissolution of the dispersed orthophosphate droplet phase. Alternatively, the strontium phosphate phase in the substituted glasses might dissolve more readily than the calcium phosphate phase in Sr0.

The initial elemental concentrations of silicon and Sr are a linear function of the square root of time (figure 4) up to about 120 min, which indicates a diffusion-controlled process. Similar release kinetics were found for ions in all the glasses studied, although there was considerable more experimental scatter on the figures for the 2.5 per cent and 10 per cent Sr glasses owing to their low Sr contents and the smaller amounts of ions released.

SBF was designed to give ionic concentrations comparable with those found in blood plasma, and initial ionic concentrations in SBF for Ca, Na and P are 2.5, 141 and 1 mmol l^{-1}, respectively. The ionic concentrations of Ca, phosphate and carbonate in SBF are close to the solubility limit of HCA; therefore, a slight change in the concentrations of these ions or a slight pH increase favour precipitation of HCA. The release of ions into SBF (figure 2) is complicated by the ions already present in SBF, but also by apatite formation, which consumes ions such as Ca^{2+}, Sr^{2+} or PO_4^{3-}, and this accounts for the differences between results for Tris buffer and SBF seen in figure 2.

After about 60 min, concentrations of silicon in SBF reach about 2.5 mmol l^{-1} (70 ppm). This is approximately the solubility limit of $Si(OH)_4$, although this varies with experimental conditions such as pH. The time point of saturation of Si in solution would be expected to correlate with the formation of a silica gel and precipitation of apatites such as HCA; however, recent experiments have shown that formation of a silica gel layer is not necessarily a prerequisite for apatite formation [19,20].

Phosphate concentrations in SBF increased initially, then dropped to near zero, which can be explained by an initial release from the glass, and subsequent depletion owing to the formation of apatite. Similarly, concentrations of Ca were affected by the release from the glass (as described earlier for Tris buffer) on the one hand and formation of apatite (and thereby consumption of Ca^{2+} ions) on the other hand, although trends were not as clear as for phosphate.

Ion release in SBF can be compared with that in cell culture media, which also contain ions in varying concentrations and also favour apatite formation [7], and further details will be discussed later, together with the results for apatite formation.

3.2. Apatite deposition in simulated body fluid

FTIR spectra of all glasses showed significant changes after immersion in Tris buffer in comparison with the spectrum of the unreacted glass (figure 5). The bands for the unreacted glass powder were mostly owing to Si–O vibrational modes [21]; after immersion in SBF, the non-bridging oxygen (Si–O^- alkali$^+$) band at 920 cm^{-1} disappeared. At the same time, new bands appeared at about 790 cm^{-1}, which were assigned to Si–O–Si bond vibration between two adjacent SiO_4 tetrahedra [18]. These changes indicate formation of a silica gel surface layer after leaching of Ca^{2+} and Na^+ ions and formation of Si-OH groups in this ion-depleted glass in agreement with ion release data.

Apatitic PO_4^{3-} groups give characteristic split bands at 560 and 600 cm^{-1} [22], with a third signal at 575 cm^{-1} [23] observed for crystallites of small size.

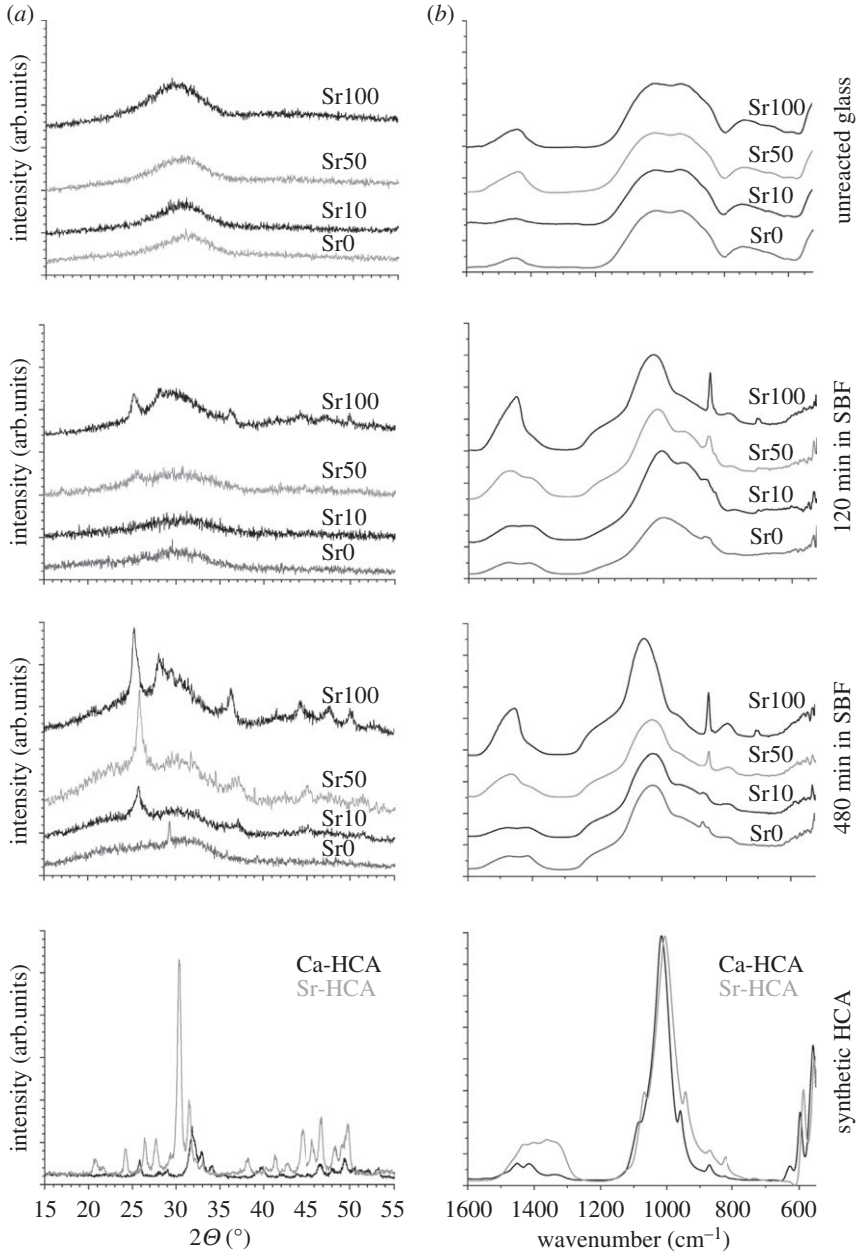

Figure 5. (*a*) XRD patterns and (*b*) FTIR spectra of untreated glass, glass powder treated in SBF for 120 and 480 min, and synthetic strontium (Sr-HCA) and calcium hydroxy-carbonate apatite (Ca-HCA).

This is the most characteristic region for apatite and other phosphates. The split bands are clearly present for synthetic strontium (Sr-HCA) and calcium hydroxy-carbonate apatite (Ca-HCA) in figure 5. A single peak in this area usually suggests the presence of non-apatitic or amorphous calcium phosphate, which is usually taken as an indication of the presence of precursors to apatite [24]. FTIR spectra of SBF-treated glasses in this study, however, do not show any bands in this region, suggesting that no or only poorly crystalline apatite has formed. Alternatively, the absence of split bands at 560 and 600 cm^{-1} may be a result of a mixed Ca/Sr-HCA being formed, and the disordered structure of such apatite may lead to broadening of the phosphate vibrational mode and the loss of this characteristic splitting.

In the FTIR spectra of the glass powders at 120 min, the proportion of the bands at 920 and 1030 cm^{-1} changes with increasing Sr content, which supports the suggestion that Sr increases the degradation rate of the glass. However, FTIR spectra of the Sr0, Sr10 and Sr50 compositions look very similar at 480 min in SBF, except for the small sharp features at 715 and 870 cm^{-1}. Both we assigned to carbonate [19] either as HCA, or as Sr/Ca carbonate, which can explain the drop in the pH of SBF mentioned already. Only the fully Sr-substituted glass Sr100 showed further degradation at this time point.

Results of powder XRD experiments of Sr-substituted glass powders treated in SBF for 8 h (480 min) showed presence of apatite peaks (HCA; JCPDS 19–272, Joint Committee on Powder Diffraction Standards, now the International Centre for Diffraction Data) at 26 and 32–34°2θ at 480 min (figure 5). Apatite peaks became more pronounced with increasing Sr for Ca substitution in the glass. It is not clear whether the

more pronounced peaks in the Sr-substituted glasses are owing to more apatite having formed or owing to the stronger scattering effect of Sr compared with Ca. Glass Sr0 did not show characteristic apatite peaks, but instead a single peak at about 29.4°2θ, which might indicate carbonate formation ($CaCO_3$; JCPDS 5–586) as suggested by FTIR analysis. Sr-containing glasses showed small peaks at 120 min, which seem to be mostly caused by strontianite ($SrCO_3$; JCPDS 5–418) or a mixed $(Ca,Sr)CO_3$ (JCPDS 44–1421). The presence of small amounts of apatite cannot be excluded, particularly as SBF was depleted of phosphate at this time point as shown in figure 2. The presence of $SrCO_3$ or mixed Sr/Ca carbonate can also explain the enhanced intensity of the 26°2θ peak of the Sr-substituted glasses after SBF treatment (480 min), which suggests overlapping peaks of apatite and carbonate. This agrees with the strong carbonate bands in the FTIR analysis as well as decreasing pH values of SBF solutions compared with Tris buffer.

Diffraction lines of apatite peaks of the SBF-treated glasses are broad compared with those of synthetic Ca-HCA and Sr-HCA, indicating the precipitated apatite to be less crystalline, and this line broadening can be explained by the following three factors:

— small, nanometer-sized crystals are known to cause line broadening in XRD, and apatite crystals formed in SBF were shown to be in the nanometer size range [25];
— solid solution formation as a result of carbonate substituting for phosphate in the lattice would be expected to result in line broadening as described earlier [18]; and
— similarly, solid solution formation as a result of formation of a mixed Ca/Sr apatite would be expected to cause line broadening.

While it is likely that the apatite formed on Sr-containing bioactive glasses in SBF is also in the nanometer size range (below 50 nm), owing to the line broadening being affected by partial substitutions in the apatite lattice, it is not possible to actually determine the crystallite size in this study.

The degradation and apatite formation of the Sr-substituted bioactive glasses in SBF has been verified by ^{31}P MAS-NMR. Figure 6*a* indicates phosphorus present as dominantly orthophosphate species in the unreacted glass (bottom spectrum) as discussed previously [13]. Sr100 after 480 min in SBF showed a main peak at 3.3 ppm with slight asymmetry on the left-hand side of the peak. We assigned this main signal at 3.3 ppm to Sr-HCA, with the asymmetry owing to the residual glass fraction. The width of the ^{31}P MAS-NMR line obtained for Sr-HCA precipitated in SBF confirms poor crystallinity of the apatite compared with synthetic Sr-HCA (top spectrum), which is consistent with the XRD and FTIR results from figure 5. In figure 6*b*, comparison between three different glass compositions treated for 480 min in SBF reveals a significant difference between glass Sr100 and Sr0. Although formation of apatite occurs for all compositions, the fraction of the residual glass remains

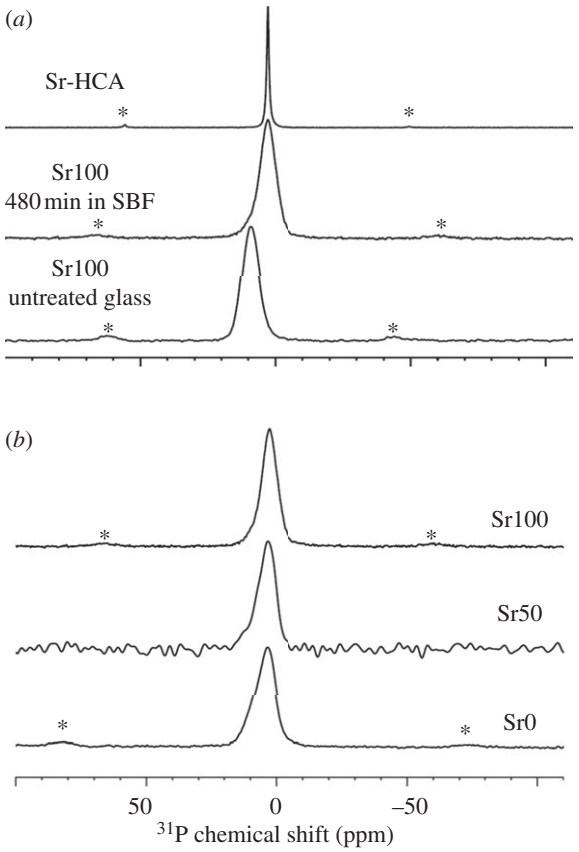

Figure 6. ^{31}P MAS-NMR spectra of (*a*) untreated glass Sr100 (bottom), Sr100 after 480 min in SBF (centre) and synthetic strontium-HCA (top), and (*b*) glass powders treated in SBF for 480 min. Asterisks (*) represent spinning side bands.

small (*ca* 5%) in the Sr100 glass only. The spectrum for Sr50 looks very similar to that of Sr0, but with a poorer signal-to-noise ratio. FTIR results also showed great similarity between the spectra of glasses Sr0–Sr50. Thus, NMR results suggest that full Sr substitution in the bioactive glass provides the combined benefits of both significantly enhanced early glass dissolution and apatite formation.

It is not quite clear how much of the Ca and phosphate for apatite formation comes from the glass and how much comes from surrounding solution (SBF). Looking at Sr-containing bioactive glasses may help elucidate the process of HCA formation. Sr forms a complete and continuous solid solution series with Ca in apatites [26,27], and thus Sr may be useful as a probe for the HCA formation process. While the fact that Sr forms complete solid solutions with Ca in apatites has been known for over 40 years, a recent erroneous study [28] suggested that only 15 per cent of the Ca can be substituted by Sr. There is also evidence that the replacement of a small fraction of Ca by Sr in the apatite crystal lattice results in a reduction in the solubility product [26]. This phenomenon is the basis of using Sr salts in remineralizing toothpastes and is the explanation why areas in the world with naturally strontiated water supplies have very low rates of dental caries [29,30].

SEM analysis of the disc samples after SBF immersion using both secondary and back-scattered electrons

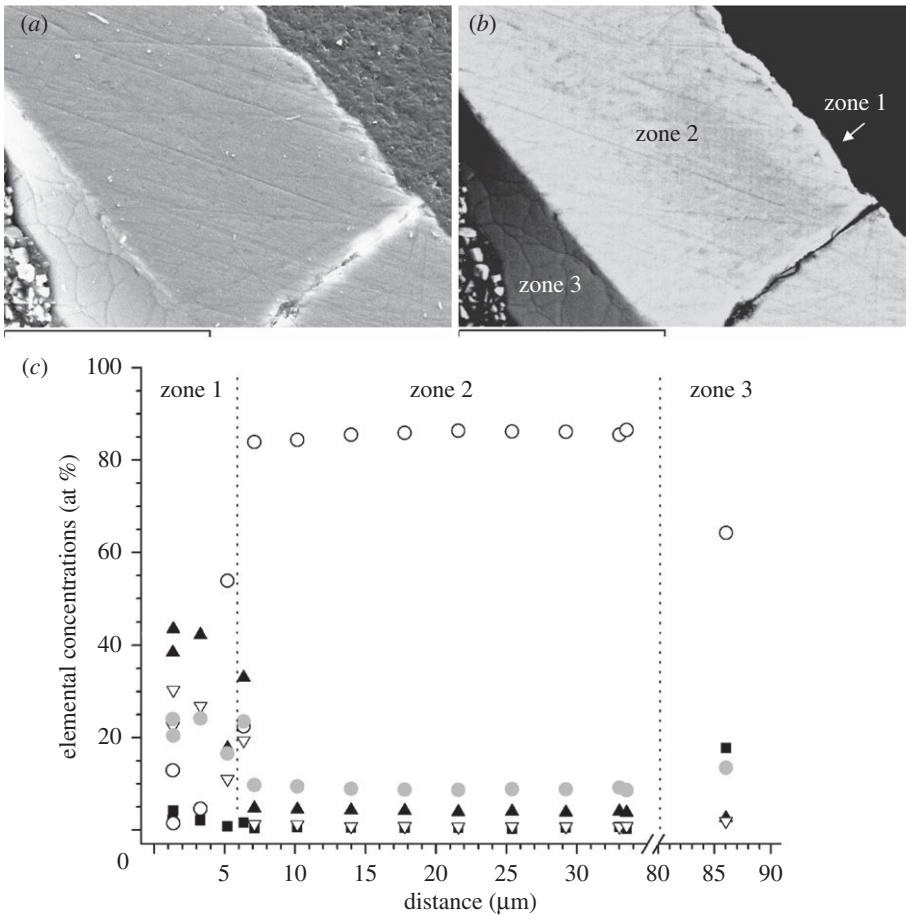

Figure 7. SEM–EDX analysis of a cross section of Sr50 disc after 1 week in SBF: (*a*) secondary electron; (*b*) back-scattered electron images (scale bars are 60 μm); (*c*) atomic composition on a straight line from zone 1 (i.e. the glass/SBF interface) to zone 3 (i.e. the unreacted glass; filled squares, Na; open circles, Si; filled triangles, P; open inverted triangles, Ca; filled grey circles, Sr).

(figure 7) shows several different zones to be distinguished. The black area corresponds to the mounting epoxy resin, which was used to embed the sample. Figure 7*b* shows a bright layer at the surface (zone 1) corresponding to the interface of the glass and the SBF, a phase with a high concentration of high atomic number elements. SEM–EDX analysis of zone 1 (figure 7*c*) shows that this phase is rich in alkaline earth ions (Sr and Ca) and in phosphorus, suggesting it to be an apatite surface layer. The (Ca + Sr)/P ratio in this zone is 1.3 ± 0.2, i.e. below the ratio in apatite of 1.67; however, we do not necessarily expect an exact stoichiometry in this biomimetic apatite [31]. The lower (Ca + Sr)/P ratio can possibly be explained by the presence of a mixture of apatite and octacalcium phosphate (Ca/P ratio 1.33), or it could be owing to carbonate (B-type) substitution in the apatite lattice (with a decrease in Ca or Sr content to compensate for CO_3^{2-} being substituted for PO_4^{3-}), which has been observed previously for bioactive glasses [20]. The next zone (zone 2) has a high silica content, whereas concentrations of P, Na, Ca and Sr are very low. This confirms the presence of the ion-depleted glass or silica gel layer. Cation concentrations in zone 3 are higher again, being closer to the original composition of glass Sr50 (table 1). Figure 7*c* shows Sr and Ca concentrations in zone 1 to be similar, reflecting the original glass composition despite the fact that only Ca is present in SBF. This suggests that the HCA layer forms from Ca and Sr initially released from the glass, rather than from the SBF. The ions released from the glass (initially controlled by diffusion; figure 4) seem to stay close to the glass surface and precipitate apatite, rather than diffusing into the SBF and then precipitating HCA from there.

3.3. *Influence on* in vitro *cell behaviour*

Bioactive glasses such as 45S5 are known to enhance cell metabolic activity [11,12,32,33]. Sr-substituted bioactive glasses have recently been shown to further enhance metabolic activity of osteoblasts compared with Sr-free bioactive glass Sr0 [7], and it was suggested that Sr ions may act synergistically with other ions (such as silicon) released from the glass. In addition, glass extracts (i.e. culture medium exposed to bioactive glass particles for defined amounts of time) were shown to inhibit osteoclast differentiation and resorption [7].

While for experiments with glass extracts only the ion release from the glass (i.e. the elemental concentrations in the culture medium) need to be considered, culture studies on glass discs are more complex to interpret. Here, both the elemental concentrations in the

medium and the surface of the substrate (such as presence or absence of nanocrystalline apatite) are known to influence cell behaviour. While the apatite-forming ability of a bioactive glass alone is not sufficient to predict cell behaviour [34], the apatite layer is known to be critical for adsorption of proteins such as vitronectin, which is a prerequisite for cell attachment and proliferation [10]. If a bioactive glass forms apatite faster, then cells can be expected to attach and, subsequently, proliferate at earlier time points, which explains the significantly higher cell numbers on Sr100 and Sr50 compared with the Sr-free glass Sr0 reported previously [7].

The combination of glass degradation and cell culture data suggests that with a thorough understanding of the composition–structure–property relationship, the glass chemistry can be tailored to release an appropriate level of Sr or other therapeutically active ions depending on the application.

3.4. Applications

Sr-releasing bioactive glasses are of interest for use in a wide range of orthopaedic applications such as bone void fillers, porous scaffolds for tissue engineering applications or coatings of metallic implants [35]. Their combined benefits of apatite formation and release of Sr ions makes them particularly interesting for use in patients suffering from osteoporosis [7]. Recently, bioactive glasses have also found application in dentistry as a remineralizing additive for toothpastes, particularly for treating dentine hypersensitivity by precipitating HCA onto the tooth surface and sealing the dentinal tubules [36,37]. Incorporation of Sr into bioactive glasses is beneficial, as Sr was shown to prevent dental caries [29], it improves enamel remineralization [38] and Sr salts (such as strontium acetate or chloride) are already used in remineralizing toothpastes. Bioactive glasses therefore have the potential to combine the beneficial effect of apatite formation with a more controlled release of Sr ions for treatment of dentine hypersensitivity and prevention of caries.

4. CONCLUSIONS

By substituting Sr for Ca on a molar base, glass degradation and apatite formation can be increased, while providing release of Sr ions, which are known to stimulate bone formation. Particularly by fully substituting Ca for Sr apatite formation is significantly enhanced. Sr-containing bioactive glasses have previously been shown to be a promising material for bone regeneration in patients suffering from osteoporosis, and as the Sr-containing glasses form apatite within less than 8 h, they are also of interest for applications in dentifrices. While bioactive glasses and their bone-bonding properties have been known for 40 years, these results show that glass design based on a thorough understanding of the structure–property relationship in these materials allows for the development of next-generation biomaterials that combine the release of therapeutic ions with the known bone-regenerating properties of bioactive glasses.

Y.F. thanks Imperial College London for the provision of a undergraduate research opportunity programme (UROP) bursary, which made this study possible.

REFERENCES

1 Kanis, J. A., Johnell, O., Oden, A., Sernbo, I., Redlund-Johnell, I., Dawson, A., De Laet, C. & Jonsson, B. 2000 Long-term risk of osteoporotic fracture in Malmö. *Osteoporosis Int.* **11**, 669–674. (doi:10.1007/s001980070064)

2 Kanis, J. A. & Johnell, O. 2005 Requirements for DXA for the management of osteoporosis in Europe. *Osteoporos. Int.* **16**, 229–238. (doi:10.1007/s00198-004-1811-2)

3 Bonnelye, E., Chabadel, A., Saltel, F. & Jurdic, P. 2008 Dual effect of strontium ranelate: stimulation of osteoblast differentiation and inhibition of osteoclast formation and resorption *in vitro*. *Bone* **42**, 129–138. (doi:10.1016/j.bone.2007.08.043)

4 Marie, P. J., Hott, M., Modrowski, D., Depollak, C., Guillemain, J., Deloffre, P. & Tsouderos, Y. 1993 An uncoupling agent containing strontium prevents bone loss by depressing bone-resorption and maintaining bone-formation in estrogen-deficient rats. *J. Bone Miner. Res.* **8**, 607–615. (doi:10.1002/jbmr.5650080512)

5 Marie, P. J. 2005 Strontium as therapy for osteoporosis. *Curr. Opin. Pharmacol.* **5**, 633–636. (doi:10.1016/j.coph.2005.05.005)

6 O'Donnell, S., Cranney, A., Wells, G. A., Adachi, J. D. & Reginster, J. Y. 2006. Strontium ranelate for preventing and treating postmenopausal osteoporosis. Report no. CD005326. Cochrane Database of Systematic Reviews.

7 Gentleman, E., Fredholm, Y. C., Jell, G., Lotfibakhshaiesh, N., O'Donnell, M. D., Hill, R. G. & Stevens, M. M. 2010 The effects of strontium-substituted bioactive glasses on osteoblasts and osteoclasts *in vitro*. *Biomaterials* **31**, 3244–3252. (doi:10.1016/j.biomaterials.2010.01.121)

8 Hench, L. L., Splinter, R. J., Allen, W. C. & Greenlee, T. K. 1971 Bonding mechanisms at the interface of ceramic prosthetic materials. *J. Biomed. Mater. Res.* **5**, 117–141. (doi:10.1002/jbm.820050611)

9 Hench, L. L. & Paschall, H. A. 1973 Direct chemical bond of bioactive glass-ceramic materials to bone and muscle. *J. Biomed. Mater. Res.* **7**, 25–42. (doi:10.1002/jbm.820070304)

10 Webster, T. J., Ergun, C., Doremus, R. H., Siegel, R. W. & Bizios, R. 2000 Specific proteins mediate enhanced osteoblast adhesion on nanophase ceramics. *J. Biomed. Mater. Res.* **51**, 475–483. (doi:10.1002/1097-4636(20000905)51:3<475::AID-JBM23>3.0.CO;2-9)

11 Foppiano, S., Marshall, S. J., Marshall, G. W., Saiz, E. & Tomsia, A. P. 2007 Bioactive glass coatings affect the behavior of osteoblast-like cells. *Acta Biomater.* **3**, 765–771. (doi:10.1016/j.actbio.2007.02.011)

12 Jell, G. & Stevens, M. M. 2006 Gene activation by bioactive glasses. *J. Mater. Sci. Mat. Med.* **17**, 997–1002. (doi:10.1007/s10856-006-0435-9)

13 Fredholm, Y. C., Karpukhina, N., Law, R. V. & Hill, R. G. 2010 Strontium containing bioactive glasses: glass structure and physical properties. *J. Non-Crystal. Solids* **356**, 2546–2551. (doi:10.1016/j.jnoncrysol.2010.06.078)

14 O'Donnell, M. D. & Hill, R. G. 2010 Influence of strontium and the importance of glass chemistry and structure when designing bioactive glasses for bone regeneration. *Acta Biomater.* **6**, 2382–2385. (doi:10.1016/j.actbio.2010.01.006)

15 Kokubo, T., Kushitani, H., Sakka, S., Kitsugi, T. & Yamamuro, T. 1990 Solutions able to reproduce *in vivo* surface–structure changes in bioactive glass–ceramic

A-W. *J. Biomed. Mater. Res.* **24**, 721–734. (doi:10.1002/jbm.820240607)
16 Zhang, D., Hupa, M. & Hupa, L. 2008 *In situ* pH within particle beds of bioactive glasses. *Acta Biomater.* **4**, 1498–1505. (doi:10.1016/j.actbio.2008.04.007)
17 Aina, V., Malavasi, G., Pla, A. F., Munaron, L. & Morterra, C. 2009 Zinc-containing bioactive glasses: surface reactivity and behaviour towards endothelial cells. *Acta Biomater.* **5**, 1211–1222. (doi:10.1016/j.actbio.2008.10.020)
18 Brauer, D. S., Karpukhina, N., O'Donnell, M. D., Law, R. V. & Hill, R. G. 2010 Fluoride-containing bioactive glasses: effect of glass design and structure on degradation, pH and apatite formation in simulated body fluid. *Acta Biomater.* **6**, 3275–3282. (doi:10.1016/j.actbio.2010.01.043)
19 Lusvardi, G., Malavasi, G., Menabue, L., Aina, V. & Morterra, C. 2009 Fluoride-containing bioactive glasses: surface reactivity in simulated body fluids solutions. *Acta Biomater.* **5**, 3548–3562. (doi:10.1016/j.actbio.2009.06.009)
20 Mneimne, M., Hill, R. G., Bushby, A. J. & Brauer, D. S. 2011 High phosphate content significantly increases apatite formation of fluoride-containing bioactive glasses. *Acta Biomater.* **7**, 1827–1834. (doi:10.1016/j.actbio.2010.11.037)
21 Kim, C. Y., Clark, A. E. & Hench, L. L. 1989 Early stages of calcium-phosphate layer formation in bioglasses. *J. Non-Crystall. Solids* **113**, 195–202. (doi:10.1016/0022-3093(89)90011-2)
22 LeGeros, R. Z., Trautz, O. R., Klein, E. & Legeros, J. P. 1969 Two types of carbonate substitution in apatite structure. *Experientia* **25**, 5–7. (doi:10.1007/BF01903856)
23 Rey, C., Combes, C., Drouet, C., Lebugle, A., Sfihi, H. & Barroug, A. 2007 Nanocrystalline apatites in biological systems: characterisation, structure and properties. *Mater. Sci. Eng. Technol.* **38**, 996–1002. (doi:10.1002/mawe.200700229)
24 Jones, J. R., Sepulveda, P. & Hench, L. L. 2001 Dose-dependent behavior of bioactive glass dissolution. *J. Biomed. Mater. Res.* **58**, 720–726. (doi:10.1002/jbm.10053)
25 O'Donnell, M. D., Watts, S. J., Hill, R. G. & Law, R. V. 2009 The effect of phosphate content on the bioactivity of soda-lime-phosphosilicate glasses. *J. Mater. Sci. Mater. Med.* **20**, 1611–1618. (doi:10.1007/s10856-009-3732-2)
26 Driessens, F. C. M. & Verbeeck, R. M. H. 1990 *Biominerals.* Boca Raton, FL: CRC Press.
27 O'Donnell, M. D., Fredholm, Y., de Rouffignac, A. & Hill, R. G. 2008 Structural analysis of a series of strontium-substituted apatites. *Acta Biomater.* **4**, 1455–1464. (doi:10.1016/j.actbio.2008.04.018)
28 Li, Z. Y., Lam, W. M., Yang, C., Xu, B., Ni, G. X., Abbah, S. A., Cheung, K. M. C., Luk, K. D. K. & Lu, W. W. 2007 Chemical composition, crystal size and lattice structural changes after incorporation of strontium into biomimetic apatite. *Biomaterials* **28**, 1452–1460. (doi:10.1016/j.biomaterials.2006.11.001)
29 Athanassouli, T. M., Papastathopoulos, D. S. & Apostolopoulos, A. X. 1983 Dental caries and strontium concentration in drinking water and surface enamel. *J. Dental Res.* **62**, 989–991. (doi:10.1177/00220345830620091501)
30 Curzon, M. E. J., Spector, P. C. & Iker, H. P. 1978 Association between strontium in drinking-water supplies and low caries prevalence in man. *Arch. Oral Biol.* **23**, 317–321. (doi:10.1016/0003-9969(78)90025-0)
31 Eichert, D., Drouet, C., Sfihia, H., Rey, C. & Combes, C. 2009 *Nanocrystalline apatite-based biomaterials.* New York, NY: Nova Science Publishers.
32 Xynos, I. D., Hukkanen, M. V. J., Batten, J. J., Buttery, L. D., Hench, L. L. & Polak, J. M. 2000 Bioglass 45S5 stimulates osteoblast turnover and enhances bone formation *in vitro*: implications and applications for bone tissue engineering. *Calcif. Tissue Int.* **67**, 321–329. (doi:10.1007/s002230001134)
33 Xynos, I. D., Edgar, A. J., Buttery, L. D. K., Hench, L. L. & Polak, J. M. 2000 Ionic products of bioactive glass dissolution increase proliferation of human osteoblasts and induce insulin-like growth factor II mRNA expression and protein synthesis. *Biochem. Biophys. Res. Commun.* **276**, 461–465. (doi:10.1006/bbrc.2000.3503)
34 Bohner, M. & Lemaitre, J. 2009 Can bioactivity be tested *in vitro* with SBF solution? *Biomaterials* **30**, 2175–2179. (doi:10.1016/j.biomaterials.2009.01.008)
35 Lotfibakhshaiesh, N., Brauer, D. S. & Hill, R. G. 2010 Bioactive glass engineered coatings for Ti6Al4V alloys: influence of strontium substitution for calcium on sintering behaviour. *J. Non-Crystal. Solids* **356**, 2583–2590. (doi:10.1016/j.jnoncrysol.2010.05.017)
36 Tai, B. J., Bian, Z., Jiang, H., Greenspan, D. C., Zhong, J., Clark, A. E. & Du, M. Q. 2006 Anti-gingivitis effect of a dentifrice containing bioactive glass (NovaMin) particulate. *J. Clin. Periodontol.* **33**, 86–91. (doi:10.1111/j.1600-051X.2005.00876.x)
37 Du, M. Q., Bian, Z., Jiang, H., Greenspan, D. C., Burwell, A. K., Zhong, J. P. & Tai, B. J. 2008 Clinical evaluation of a dentifrice containing calcium sodium phosphosilicate (NovaMin) for the treatment of dentin hypersensitivity. *Am. J. Dentistry* **21**, 210–214.
38 Thuy, T. T. *et al.* 2008 Effect of strontium in combination with fluoride on enamel remineralization *in vitro*. *Arch. Oral Biol.* **53**, 1017–1022. (doi:10.1016/j.archoralbio.2008.06.005)